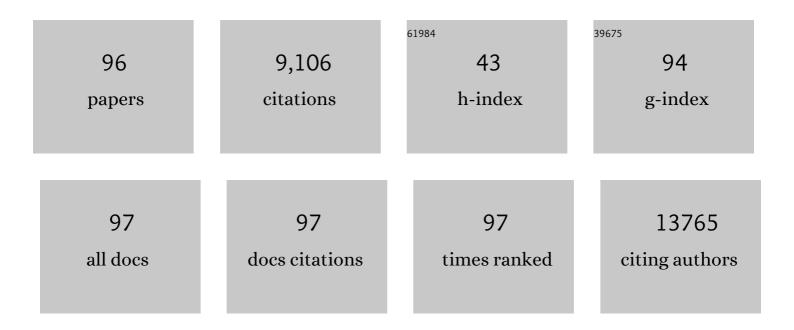
## Yeonwoong Jung

List of Publications by Year in descending order

Source: https://exaly.com/author-pdf/498858/publications.pdf Version: 2024-02-01



#	Article	IF	CITATIONS
1	Recent Advances in Two-Dimensional Materials beyond Graphene. ACS Nano, 2015, 9, 11509-11539.	14.6	2,069
2	Asymmetric Supercapacitor Electrodes and Devices. Advanced Materials, 2017, 29, 1605336.	21.0	1,021
3	Recent Advances in Two-Dimensional Nanomaterials for Supercapacitor Electrode Applications. ACS Energy Letters, 2018, 3, 482-495.	17.4	618
4	Highly scalable non-volatile and ultra-low-power phase-change nanowire memory. Nature Nanotechnology, 2007, 2, 626-630.	31.5	389
5	Metal Seed Layer Thickness-Induced Transition From Vertical to Horizontal Growth of MoS <sub>2</sub> and WS <sub>2</sub> . Nano Letters, 2014, 14, 6842-6849.	9.1	251
6	High-Performance One-Body Core/Shell Nanowire Supercapacitor Enabled by Conformal Growth of Capacitive 2D WS <sub>2</sub> Layers. ACS Nano, 2016, 10, 10726-10735.	14.6	209
7	Recent trends in transition metal dichalcogenide based supercapacitor electrodes. Nanoscale Horizons, 2019, 4, 840-858.	8.0	207
8	Record High Efficiency Single-Walled Carbon Nanotube/Silicon p <i>–</i> n Junction Solar Cells. Nano Letters, 2013, 13, 95-99.	9.1	193
9	Intercalation in two-dimensional transition metal chalcogenides. Inorganic Chemistry Frontiers, 2016, 3, 452-463.	6.0	181
10	Synthesis and Structural Characterization of Single-Crystalline Branched Nanowire Heterostructures. Nano Letters, 2007, 7, 264-268.	9.1	165
11	One-Step Synthesis of MoS <sub>2</sub> /WS <sub>2</sub> Layered Heterostructures and Catalytic Activity of Defective Transition Metal Dichalcogenide Films. ACS Nano, 2016, 10, 2004-2009.	14.6	164
12	Electrical Wind Force–Driven and Dislocation-Templated Amorphization in Phase-Change Nanowires. Science, 2012, 336, 1561-1566.	12.6	162
13	Two-dimensional transition metal dichalcogenide hybrid materials for energy applications. Nano Today, 2018, 19, 16-40.	11.9	142
14	Size-dependent phase transition memory switching behavior and low writing currents in GeTe nanowires. Applied Physics Letters, 2006, 89, 223116.	3.3	116
15	Centimeter Scale Patterned Growth of Vertically Stacked Few Layer Only 2D MoS2/WS2 van der Waals Heterostructure. Scientific Reports, 2016, 6, 25456.	3.3	116
16	Synthesis and Characterization of Ge2Sb2Te5Nanowires with Memory Switching Effect. Journal of the American Chemical Society, 2006, 128, 14026-14027.	13.7	111
17	Coreâ~'Shell Heterostructured Phase Change Nanowire Multistate Memory. Nano Letters, 2008, 8, 2056-2062.	9.1	103
18	Extremely low drift of resistance and threshold voltage in amorphous phase change nanowire devices. Applied Physics Letters, 2010, 96, .	3.3	91

#	Article	IF	CITATIONS
19	Improved efficiency of smooth and aligned single walled carbon nanotube/silicon hybrid solar cells. Energy and Environmental Science, 2013, 6, 879.	30.8	87
20	A leaf-inspired photon management scheme using optically tuned bilayer nanoparticles for ultra-thin and highly efficient photovoltaic devices. Nano Energy, 2019, 58, 47-56.	16.0	86
21	Strain Effect in Palladium Nanostructures as Nanozymes. Nano Letters, 2020, 20, 272-277.	9.1	85
22	Experimental Realization of Few Layer Two-Dimensional MoS <sub>2</sub> Membranes of Near Atomic Thickness for High Efficiency Water Desalination. Nano Letters, 2019, 19, 5194-5204.	9.1	80
23	Horizontal-to-Vertical Transition of 2D Layer Orientation in Low-Temperature Chemical Vapor Deposition-Grown PtSe <sub>2</sub> and Its Influences on Electrical Properties and Device Applications. ACS Applied Materials & Interfaces, 2019, 11, 13598-13607.	8.0	77
24	Synthesis of SnTe Nanoplates with {100} and {111} Surfaces. Nano Letters, 2014, 14, 4183-4188.	9.1	75
25	Novel mesoporous electrode materials for symmetric, asymmetric and hybrid supercapacitors. Nanotechnology, 2019, 30, 202001.	2.6	75
26	Nanowire Transformation by Size-Dependent Cation Exchange Reactions. Nano Letters, 2010, 10, 149-155.	9.1	74
27	Improving Electrochemical Pb <sup>2+</sup> Detection Using a Vertically Aligned 2D MoS <sub>2</sub> Nanofilm. Analytical Chemistry, 2019, 91, 11770-11777.	6.5	73
28	Size-Dependent Surface-Induced Heterogeneous Nucleation Driven Phase-Change in Ge2Sb2Te5 Nanowires. Nano Letters, 2008, 8, 3303-3309.	9.1	72
29	Chemically Synthesized Heterostructures of Two-Dimensional Molybdenum/Tungsten-Based Dichalcogenides with Vertically Aligned Layers. ACS Nano, 2014, 8, 9550-9557.	14.6	70
30	Artificial Neuron using Vertical MoS2/Graphene Threshold Switching Memristors. Scientific Reports, 2019, 9, 53.	3.3	69
31	A Library of Atomically Thin 2D Materials Featuring the Conductiveâ€Point Resistive Switching Phenomenon. Advanced Materials, 2021, 33, e2007792.	21.0	67
32	Nanoscale size effects in crystallization of metallic glass nanorods. Nature Communications, 2015, 6, 8157.	12.8	65
33	2D MoS <sub>2</sub> -Based Threshold Switching Memristor for Artificial Neuron. IEEE Electron Device Letters, 2020, 41, 936-939.	3.9	64
34	Strength dependence of epoxy composites on the average filler size of non-oxidized graphene flake. Carbon, 2017, 113, 379-386.	10.3	63
35	Multifunctional Two-Dimensional PtSe <sub>2</sub> -Layer Kirigami Conductors with 2000% Stretchability and Metallic-to-Semiconducting Tunability. Nano Letters, 2019, 19, 7598-7607.	9.1	59
36	High-Resolution Transmission Electron Microscopy Study of Electrically-Driven Reversible Phase Change in Ge <sub>2</sub> Sb <sub>2</sub> Te <sub>5</sub> Nanowires. Nano Letters, 2011, 11, 1364-1368.	9.1	58

#	Article	IF	CITATIONS
37	Electronic synapses with near-linear weight update using MoS2/graphene memristors. Applied Physics Letters, 2019, 115, .	3.3	52
38	Noble metal-coated MoS2 nanofilms with vertically-aligned 2D layers for visible light-driven photocatalytic degradation of emerging water contaminants. Scientific Reports, 2017, 7, 14944.	3.3	51
39	Thickness-Independent Semiconducting-to-Metallic Conversion in Wafer-Scale Two-Dimensional PtSe <sub>2</sub> Layers by Plasma-Driven Chalcogen Defect Engineering. ACS Applied Materials & Interfaces, 2020, 12, 14341-14351.	8.0	51
40	Wafer-Scale Growth of 2D PtTe <sub>2</sub> with Layer Orientation Tunable High Electrical Conductivity and Superior Hydrophobicity. ACS Applied Materials & Interfaces, 2020, 12, 10839-10851.	8.0	48
41	Two-dimensional lateral heterojunction through bandgap engineering of MoS <sub>2</sub> via oxygen plasma. Journal of Physics Condensed Matter, 2016, 28, 364002.	1.8	47
42	Multiwavelength Optoelectronic Synapse with 2D Materials for Mixed-Color Pattern Recognition. ACS Nano, 2022, 16, 10188-10198.	14.6	47
43	Two-Dimensional/Three-Dimensional Schottky Junction Photovoltaic Devices Realized by the Direct CVD Growth of vdW 2D PtSe <sub>2</sub> Layers on Silicon. ACS Applied Materials & Interfaces, 2019, 11, 27251-27258.	8.0	46
44	Multipurpose and Reusable Ultrathin Electronic Tattoos Based on PtSe <sub>2</sub> and PtTe <sub>2</sub> . ACS Nano, 2021, 15, 2800-2811.	14.6	46
45	Centimeter-scale Green Integration of Layer-by-Layer 2D TMD vdW Heterostructures on Arbitrary Substrates by Water-Assisted Layer Transfer. Scientific Reports, 2019, 9, 1641.	3.3	44
46	Two-Dimensional Near-Atom-Thickness Materials for Emerging Neuromorphic Devices and Applications. IScience, 2020, 23, 101676.	4.1	44
47	MoS <sub>2</sub> Synapses with Ultra-low Variability and Their Implementation in Boolean Logic. ACS Nano, 2022, 16, 2866-2876.	14.6	38
48	Phase-Change Geâ^'Sb Nanowires: Synthesis, Memory Switching, and Phase-Instability. Nano Letters, 2009, 9, 2103-2108.	9.1	37
49	Artificial Nociceptor Using 2D MoS <sub>2</sub> Threshold Switching Memristor. IEEE Electron Device Letters, 2020, 41, 1440-1443.	3.9	37
50	Comparative study of memory-switching phenomena in phase change GeTe and Ge2Sb2Te5 nanowire devices. Physica E: Low-Dimensional Systems and Nanostructures, 2008, 40, 2474-2480.	2.7	36
51	Device Area Scaleâ€Up and Improvement of SWNT/Si Solar Cells Using Silver Nanowires. Advanced Energy Materials, 2014, 4, 1400186.	19.5	35
52	Strainâ€Driven and Layerâ€Numberâ€Dependent Crossover of Growth Mode in van der Waals Heterostructures: 2D/2D Layerâ€Byâ€Layer Horizontal Epitaxy to 2D/3D Vertical Reorientation. Advanced Materials Interfaces, 2018, 5, 1800382.	3.7	35
53	Vertically Aligned 2D MoS <sub>2</sub> Layers with Strain-Engineered Serpentine Patterns for High-Performance Stretchable Gas Sensors: Experimental and Theoretical Demonstration. ACS Applied Materials & Interfaces, 2020, 12, 53174-53183.	8.0	35
54	Minority Carrier Lifetimes and Surface Effects in VLSâ€Grown Axial p–n Junction Silicon Nanowires. Advanced Materials, 2011, 23, 4306-4311.	21.0	32

#	Article	IF	CITATIONS
55	Tailoring crystallization phases in metallic glass nanorods via nucleus starvation. Nature Communications, 2017, 8, 1980.	12.8	31
56	Three dimensionally-ordered 2D MoS <sub>2</sub> vertical layers integrated on flexible substrates with stretch-tunable functionality and improved sensing capability. Nanoscale, 2018, 10, 17525-17533.	5.6	31
57	Wafer-Scale Two-Dimensional MoS <sub>2</sub> Layers Integrated on Cellulose Substrates Toward Environmentally Friendly Transient Electronic Devices. ACS Applied Materials & Interfaces, 2020, 12, 25200-25210.	8.0	31
58	Uniform Vapor-Pressure-Based Chemical Vapor Deposition Growth of MoS <sub>2</sub> Using MoO <sub>3</sub> Thin Film as a Precursor for Coevaporation. ACS Omega, 2018, 3, 18943-18949.	3.5	30
59	Extraordinary Enhancement of UV Absorption in TiO <sub>2</sub> Nanoparticles Enabled by Low-Oxidized Graphene Nanodots. Journal of Physical Chemistry C, 2018, 122, 12114-12121.	3.1	30
60	Supercluster-coupled crystal growth in metallic glass forming liquids. Nature Communications, 2019, 10, 915.	12.8	30
61	Investigating 2D WS <sub>2</sub> supercapacitor electrode performance by Kelvin probe force microscopy. Journal of Materials Chemistry A, 2020, 8, 12699-12704.	10.3	29
62	High-performance flexible asymmetric supercapacitor based on rGO anode and WO <sub>3</sub> /WS <sub>2</sub> core/shell nanowire cathode. Nanotechnology, 2020, 31, 435405.	2.6	29
63	Epitaxial Growth and Ordering of GeTe Nanowires on Microcrystals Determined by Surface Energy Minimization. Nano Letters, 2009, 9, 2395-2401.	9.1	28
64	Centimeter-Scale 2D van der Waals Vertical Heterostructures Integrated on Deformable Substrates Enabled by Gold Sacrificial Layer-Assisted Growth. Nano Letters, 2017, 17, 6157-6165.	9.1	28
65	Silicon nanowires: electron holography studies of doped p–n junctions and biased Schottky barriers. Nanotechnology, 2013, 24, 115703.	2.6	27
66	Scalable Van der Waals Two-Dimensional PtTe <sub>2</sub> Layers Integrated onto Silicon for Efficient Near-to-Mid Infrared Photodetection. ACS Applied Materials & Interfaces, 2021, 13, 15542-15550.	8.0	27
67	Diameter-Controlled Synthesis of Phase-Change Germanium Telluride Nanowires via the Vaporâ^'Liquidâ `'Solid Mechanism. Journal of Physical Chemistry C, 2009, 113, 6898-6901.	3.1	25
68	Automated Assembly of Wafer-Scale 2D TMD Heterostructures of Arbitrary Layer Orientation and Stacking Sequence Using Water Dissoluble Salt Substrates. Nano Letters, 2020, 20, 3925-3934.	9.1	25
69	Surface effects on electronic transport of 2D chalcogenide thin films and nanostructures. Nano Convergence, 2014, 1, 18.	12.1	24
70	Wafer-scale 2D PtTe <sub>2</sub> layers for high-efficiency mechanically flexible electro-thermal smart window applications. Nanoscale, 2020, 12, 10647-10655.	5.6	22
71	Large-area 2D TMD layers for mechanically reconfigurable electronic devices. Journal Physics D: Applied Physics, 2020, 53, 313002.	2.8	22
72	Centimeter-Scale Periodically Corrugated Few-Layer 2D MoS <sub>2</sub> with Tensile Stretch-Driven Tunable Multifunctionalities. ACS Applied Materials & Interfaces, 2018, 10, 30623-30630.	8.0	21

#	Article	IF	CITATIONS
73	Wafer-scale 2D PtTe2 layers-enabled Kirigami heaters with superior mechanical stretchability and electro-thermal responsiveness. Applied Materials Today, 2020, 20, 100718.	4.3	21
74	Cu–Ag Alloy Nanoparticles in Hydrogel Nanofibers for the Catalytic Reduction of Organic Compounds. ACS Applied Nano Materials, 2021, 4, 6045-6056.	5.0	21
75	A Generic Approach for Embedded Catalyst-Supported Vertically Aligned Nanowire Growth. Nano Letters, 2008, 8, 1328-1334.	9.1	20
76	Large-area 2D PtTe2/silicon vertical-junction devices with ultrafast and high-sensitivity photodetection and photovoltaic enhancement by integrating water droplets. Nanoscale, 2020, 12, 23116-23124.	5.6	20
77	Chalcogenide phase-change memory nanotubes for lower writing current operation. Nanotechnology, 2011, 22, 254012.	2.6	18
78	Charge Transfer from Carbon Nanotubes to Silicon in Flexible Carbon Nanotube/Silicon Solar Cells. Small, 2017, 13, 1702387.	10.0	18
79	Superhydrophobic MoS2-based multifunctional sponge for recovery and detection of spilled oil. Current Applied Physics, 2020, 20, 344-351.	2.4	16
80	Structural Evolutions of Vertically Aligned Two-Dimensional MoS <sub>2</sub> Layers Revealed by in Situ Heating Transmission Electron Microscopy. Journal of Physical Chemistry C, 2019, 123, 27843-27853.	3.1	13
81	Controllable synthesis of platinum diselenide (PtSe <sub>2</sub> ) inorganic fullerene. Journal of Materials Chemistry A, 2020, 8, 18925-18932.	10.3	12
82	Manufacturing strategies for wafer-scale two-dimensional transition metal dichalcogenide heterolayers. Journal of Materials Research, 2020, 35, 1350-1368.	2.6	12
83	Layer Orientation-Engineered Two-Dimensional Platinum Ditelluride for High-Performance Direct Alcohol Fuel Cells. ACS Energy Letters, 2021, 6, 3481-3487.	17.4	12
84	Nanoscopically Flat Open-Ended Single-Walled Carbon Nanotube Substrates for Continued Growth. Nano Letters, 2007, 7, 15-21.	9.1	10
85	Revealing Pt-seed-induced structural effects to tribological/electrical/thermoelectric modulations in two-dimensional PtSe2 using scanning probe microscopy. Nano Energy, 2022, 91, 106693.	16.0	9
86	2D MoS2-polyurethane sponge for solar-to-thermal energy conversion in environmental applications: Crude oil recovery and seawater desalination. Journal of Water Process Engineering, 2022, 47, 102665.	5.6	9
87	Mapping of near field light and fabrication of complex nanopatterns by diffraction lithography. Nanotechnology, 2012, 23, 045301.	2.6	7
88	Mechanically rollable photodetectors enabled by centimetre-scale 2D MoS2 layer/TOCN composites. Nanoscale Advances, 2021, 3, 3028-3034.	4.6	5
89	Atomic-scale characterization of structural heterogeny in 2D TMD layers. Materials Advances, 2022, 3, 1401-1414.	5.4	5
90	Peel-and-Stick Integration of Atomically Thin Nonlayered PtS Semiconductors for Multidimensionally Stretchable Electronic Devices. ACS Applied Materials & Interfaces, 2022, 14, 20268-20279.	8.0	5

#	Article	IF	CITATIONS
91	Waferâ€&cale Van der Waals Assembly of Freeâ€&tanding Near Atom Thickness Heteroâ€Membranes for Flexible Photoâ€Detectors. Advanced Electronic Materials, 2021, 7, 2100395.	5.1	4
92	Soft Biomorph Actuators Enabled by Waferâ€Scale Ultrathin 2D PtTe <sub>2</sub> Layers. Advanced Materials Technologies, 2022, 7, 2100639.	5.8	4
93	A Case of Metastatic Uterine Tumor Originating from Small-Cell Lung Cancer (SCLC) Mimicking Uterine Sarcoma. Case Reports in Obstetrics and Gynecology, 2021, 2021, 1-4.	0.3	3
94	Electromechanical properties of individual single-walled carbon nanotubes grown on focused-ion-beam patterned substrates. Ultramicroscopy, 2009, 109, 167-171.	1.9	2
95	Supercapacitors: Asymmetric Supercapacitor Electrodes and Devices (Adv. Mater. 21/2017). Advanced Materials, 2017, 29, .	21.0	2
96	Supercluster-Coupled Crystal Growth in Metallic Glass Forming Liquids. Microscopy and Microanalysis, 2019, 25, 1410-1411.	0.4	0